

## Research Article

# Trajectories and Singular Points of Two-Dimensional Fractional-Order Autonomous Systems

Bohui Yang,<sup>1</sup> Ziyang Luo,<sup>1</sup> Xindong Zhang ,<sup>1</sup> Quan Tang,<sup>1</sup> and Juan Liu<sup>2</sup>

<sup>1</sup>School of Mathematical Sciences, Xinjiang Normal University, Urumqi, Xinjiang 830017, China

<sup>2</sup>College of Big Data Statistics, Guizhou University of Finance and Economics, Guiyang 550025, China

Correspondence should be addressed to Xindong Zhang; liaoyuan1126@163.com

Received 23 March 2022; Revised 25 June 2022; Accepted 8 July 2022; Published 28 July 2022

Academic Editor: Mohammad Alomari

Copyright © 2022 Bohui Yang et al. This is an open access article distributed under the Creative Commons Attribution License, which permits unrestricted use, distribution, and reproduction in any medium, provided the original work is properly cited.

In this paper, we study the trajectories and singular points of two-dimensional fractional-order planar autonomous linear system involving the Caputo-Fabrizio fractional derivative. By the corresponding fractional integral of the Caputo-Fabrizio fractional derivative, we obtain the analytical solutions for the fractional-order planar autonomous linear system, and then, we discuss the behavior of the trajectories for the mentioned autonomous linear system. Furthermore, we consider the existence of singular points in the trajectories. We discuss the conditions under which the singular point is stable or unstable. By determining the value range of the parameters, we obtain the theorems on the type of singular points. Finally, some examples are given to verify the analysis for the mentioned autonomous linear system.

## 1. Introduction

A fractional differential equation is an equation which contains fractional derivatives. There are many forms of fractional derivatives, such as the Riemann-Liouville, Grünwald-Letnikov, and Caputo fractional derivatives. Podlubny summarized and studied the basic theory of fractional differential and fractional differential equation in [1]. About fractional differential equation, there are many results; Albadarneh et al. [2, 3] considered the numerical approach of the Riemann-Liouville and Caputo fractional derivative operators. Lin and Xu [4] studied the finite difference/spectral approximation of time fractional diffusion equations. Zhuang et al. [5] studied the numerical method of variable-order fractional advection diffusion equation with nonlinear source term. Nieto studied numerical solutions of fractional logistic ordinary differential equations in [6]. Liu et al. studied the RBF-FD semidiscrete numerical solution of time fractional convection diffusion equation in [7]. It has been found that the behavior of many physical systems can be properly described by using the fractional-order system theory. A fractional-order system means a system described by a fractional differential equation or fractional integral equation or

a system of such equations. There are many results about autonomous systems; one can refer to [8–11]. Meanwhile, the fractional-order systems have been studied by many scholars; for example, Albadarneh et al. studied the analytical solutions of linear and nonlinear incommensurate fractional-order coupled systems in [12]. Ahmad and Harb considered autonomous chaotic systems of integer and fractional orders in [13]. Li and Chen studied the fractional-order Chen system and its control in [14]. Kingni et al. considered three-dimensional chaotic autonomous system and its fractional-order form in [15]. In [16], Caputo and Fabrizio present a new definition of fractional derivative with a smooth kernel. Losada and Nieto studied the properties of a new fractional derivatives without singular kernels in [17], and they also studied the special cases of the Caputo-Fabrizio and Atangana-Baleanu derivatives in [18]. Akman et al. studied the new discretization scheme of the Caputo-Fabrizio derivatives in [19]. Xu and Jian considered unsteady rotating electroosmotic flow with the time-fractional Caputo-Fabrizio derivative in [20]. Caputo and Fabrizio [21] focused on the applications of the Caputo-Fabrizio derivative to partial differential equation. Owolabi studied the calculation and analysis of the Caputo-Fabrizio derivatives of pseudoflat algae

species model in [22]. Haq et al. studied a new approach for the qualitative study of vector born disease using the Caputo-Fabrizio derivative in [23]. Fardi and Khan proposed a finite difference spectral method for moving/nonmoving fractal transport model based on the Caputo-Fabrizio fractional derivative in [24]. Harrouche et al. considered the computational algorithm for solving uncertain pharmacokinetic models with the nonsingular nuclear Caputo-Fabrizio fractional derivative in [25]. In [26], Zhang and Li considered the exponential Euler schemes for the Caputo-Fabrizio fractional-order differential equations with multiple delays.

In this paper, we consider the Caputo-Fabrizio fractional-order planar autonomous real linear system. The two-dimensional fractional-order autonomous system is of the form

$$\mathcal{D}_t^\alpha X(t) = AX(t) \text{ or } \begin{cases} \mathcal{D}_t^\alpha x(t) = a_{11}x(t) + a_{12}y(t), \\ \mathcal{D}_t^\alpha y(t) = a_{21}x(t) + a_{22}y(t), \end{cases} \quad (1)$$

where

$$\begin{aligned} 0 < \alpha < 1, \\ X(t) &= \begin{pmatrix} x(t) \\ y(t) \end{pmatrix}, \\ A &= \begin{pmatrix} a_{11} & a_{12} \\ a_{21} & a_{22} \end{pmatrix}. \end{aligned} \quad (2)$$

The fractional derivative  $\mathcal{D}_t^\alpha x(t)$  is the Caputo-Fabrizio fractional derivative with  $0 < \alpha < 1$ , defined as (one can see [16])

$$\mathcal{D}_t^\alpha x(t) = \frac{1}{1-\alpha} \int_0^t e^{-\alpha(t-s)/(1-\alpha)} x'(s) ds. \quad (3)$$

For the Caputo-Fabrizio fractional derivative, the corresponding fractional integral of a function  $x(t)$  is that

$$\mathcal{I}_t^\alpha x(t) = (1-\alpha)[x(t) - x(0)] + \alpha \int_0^t x(s) ds, \quad (4)$$

where  $x(0)$  is the initial condition; one can refer to [17]. Thus, we have

$$\mathcal{I}_t^\alpha \mathcal{D}_t^\alpha x(t) = x(t) + c, \quad (5)$$

where  $c$  is an arbitrary constant.

The main interest in studying (1) is twofold: the first one is that a large number of dynamic processes in applied sciences are governed by such systems; the second one is that the qualitative behavior of its solutions can be illustrated through the geometry in the  $xy$ -plane.

The results for trajectories and singular points can be found in [27–29]. To the best of our knowledge, the only known example of fractional-order dynamical systems for trajectories and singular points can be found in [27], where the fractional derivative is in the Caputo sense. And similar

results of fractional-order autonomous systems with the Caputo-Fabrizio fractional derivative have not been found. The main goal of this paper is to study the trajectories and singular points of two-dimensional fractional-order planar autonomous linear systems, where the fractional derivative is in the Caputo-Fabrizio sense. In our paper, the undefined terms and notation will follow [8, 10].

## 2. Solution of Fractional Planar Autonomous Linear Systems

In this section, we consider fractional-order planar real linear system (1) under the assumption that  $\det(A) \neq 0$ . We know that system (1) has a unique singular point  $O(0, 0)$  if and only if  $\det(A) \neq 0$ . By the analysis in [30], we know that system (1) will become

$$\mathcal{D}_t^\alpha \tilde{X}(t) = T^{-1}AT\tilde{X}(t) = B\tilde{X}(t), \quad (6)$$

where  $T$  is a nonsingular matrix,  $X(t) = T\tilde{X}(t)$ , and  $\tilde{X}(t) = [u(t), v(t)]^T$ . And  $B = T^{-1}AT$  is one of the following normal forms:

$$\begin{aligned} \mathcal{L}(\lambda, \mu) &= \begin{pmatrix} \lambda & 0 \\ 0 & \mu \end{pmatrix}, \\ \mathcal{M}(\lambda) &= \begin{pmatrix} \lambda & 0 \\ 1 & \lambda \end{pmatrix}, \\ \mathcal{R}(\eta, \gamma) &= \begin{pmatrix} \eta & \gamma \\ -\gamma & \eta \end{pmatrix}. \end{aligned} \quad (7)$$

Here,  $\lambda, \mu, \eta$  and  $\gamma$  are real numbers with  $\mu \neq 0$  and  $\gamma > 0$ . The above three cases are denoted by  $\mathcal{L}$  for left,  $\mathcal{M}$  for middle, and  $\mathcal{R}$  for right, respectively. If  $p^2 - 4q > 0$ , we have the real case  $\mathcal{L}$ . If  $p^2 - 4q < 0$ , we have the complex case  $\mathcal{R}$ . If  $p^2 - 4q = 0$ , the case  $\mathcal{L}$  or  $\mathcal{M}$  occurs depending on whether  $\lambda = \mu$  has two linearly independent eigenvectors.

If  $\det(A) \neq 0$  and  $a_{12} = a_{21} = 0$ , system (1) will become (6) with case  $\mathcal{L}$ . Next, we mainly consider the solution of system (1) for the case  $\mathcal{L}$ . This implies that  $\lambda = a_{11}$  and  $\mu = a_{22}$ . Thus, system (1) will become

$$\begin{cases} \mathcal{D}_t^\alpha x(t) = \lambda x(t), \\ \mathcal{D}_t^\alpha y(t) = \mu y(t). \end{cases} \quad (8)$$

Observe that for  $\alpha = 1$ , system (8) is recovered to the classical autonomous system as follows:

$$\begin{cases} x'(t) = \lambda x(t), \\ y'(t) = \mu y(t), \end{cases} \quad (9)$$

which has the solutions  $x(t) = c_1 e^{\lambda t}$  and  $y(t) = c_2 e^{\mu t}$ .

For  $A = \mathcal{L}(\lambda, \mu)$ , the following theorem can be obtained.

**Theorem 1.** Let  $x_0$  and  $y_0$  be the initial conditions of system (8); by (4) and (5), we get the solutions of system (8) which are  $x(t) = c_1 e^{(\lambda\alpha/(1-\lambda+\lambda\alpha))t}$  and  $y(t) = c_2 e^{(\mu\alpha/(1-\mu+\mu\alpha))t}$ , where  $c_1 = x_0$  and  $c_2 = y_0$ .

*Proof.* Let  $x(t)$  and  $y(t)$  be the solutions of (8). By (4) and (5), we get that

$$\begin{cases} x(t) + c_1 = \lambda \mathcal{I}_t^\alpha x(t) = \lambda(1 - \alpha)[x(t) - x(0)] + \lambda\alpha \int_0^t x(s) ds, \\ y(t) + c_2 = \mu \mathcal{I}_t^\alpha y(t) = \mu(1 - \alpha)[y(t) - y(0)] + \mu\alpha \int_0^t y(s) ds. \end{cases} \quad (10)$$

Taking the first derivative both sides of (10), we get

$$\begin{cases} x'(t) = \lambda(1 - \alpha)x'(t) + \lambda\alpha x(t), \\ y'(t) = \mu(1 - \alpha)y'(t) + \mu\alpha y(t). \end{cases} \quad (11)$$

By (11), for  $1 - \lambda + \lambda\alpha \neq 0$  and  $1 - \mu + \mu\alpha \neq 0$ , the analytical solutions of system (8) with  $0 < \alpha < 1$  are given by

$$\begin{cases} x(t) = c_1 e^{\lambda\alpha t/(1-\lambda+\lambda\alpha)}, \\ y(t) = c_2 e^{\mu\alpha t/(1-\mu+\mu\alpha)}, \end{cases} \quad (12)$$

where  $c_1 = x_0$  and  $c_2 = y_0$  are real constants. □

If  $A = \mathcal{M}(\lambda)$ , then system (1) will become as follows:

$$\begin{cases} \mathcal{D}_t^\alpha x(t) = \lambda x(t), \\ \mathcal{D}_t^\alpha y(t) = x(t) + \lambda y(t). \end{cases} \quad (13)$$

Observe that for  $\alpha = 1$ , system (13) is recovered to the classical autonomous system as follows:

$$\begin{cases} x'(t) = \lambda x(t), \\ y'(t) = x(t) + \lambda y(t). \end{cases} \quad (14)$$

Similar with the case  $A = \mathcal{L}(\lambda, \mu)$ , we can get the following theorem for  $A = \mathcal{M}(\lambda)$ .

**Theorem 2.** Let  $x_0$  and  $y_0$  be the initial conditions of system (13); then, the solutions of system (13) are  $x(t) = c_1 e^{(\lambda\alpha/(1-\lambda+\lambda\alpha))t}$  and  $y(t) = (c_1 \alpha t / (1 - \lambda + \lambda\alpha)^2 + c_2) e^{(\lambda\alpha/(1-\lambda+\lambda\alpha))t}$ , where  $c_1 = x_0$  and  $c_2 = y_0$ .

If  $A = \mathcal{R}(\eta, \gamma)$ , then system (1) will become as follows:

$$\begin{cases} \mathcal{D}_t^\alpha x(t) = \eta x(t) + \gamma y(t), \\ \mathcal{D}_t^\alpha y(t) = -\gamma x(t) + \eta y(t). \end{cases} \quad (15)$$

Observe that for  $\alpha = 1$ , system (15) is recovered to the classical autonomous system as follows:

$$\begin{cases} x'(t) = \eta x(t) + \gamma y(t), \\ y'(t) = -\gamma x(t) + \eta y(t). \end{cases} \quad (16)$$

Similar with the case  $A = \mathcal{L}(\lambda, \mu)$ , we can get the following theorem for  $A = \mathcal{R}(\eta, \gamma)$ .

**Theorem 3.** Let  $x_0$  and  $y_0$  be the initial conditions of system (15). Then, the solutions of system (15) are  $x(t) = c_1 e^{\eta_1 t} \cos(-\gamma_1 t + c_2)$  and  $y(t) = c_1 e^{\eta_1 t} \sin(-\gamma_1 t + c_2)$ , where  $\eta_1 = (\eta\alpha - (\alpha - \alpha^2)(\eta^2 + \gamma^2)) / ((1 - \eta + \eta\alpha)^2 + (\gamma - \gamma\alpha)^2)$  and  $\gamma_1 = \gamma\alpha / ((1 - \eta + \eta\alpha)^2 + (\gamma - \gamma\alpha)^2)$ , and  $c_1, c_2$  satisfy that  $x_0 = c_1 \cos c_2$  and  $y_0 = c_1 \sin c_2$ .

### 3. Singular Points in the Solution Trajectories

In this section, we discuss the trajectories and singular points of (8), (13), and (15), respectively. Since  $\det(A) \neq 0$ , then  $O(0, 0)$  is the unique singular point of (8), (13), and (15). Further, we investigate the distribution of trajectories in the neighborhood of point  $O(0, 0)$ . By (11), we know that  $x = 0$  and  $y = 0$  are the trajectories of (8), respectively (strictly speaking,  $x = 0$  contains three trajectories:  $x = 0, y > 0$ ,  $x = 0, y < 0$ , and  $x = 0, y = 0$ ; for convenience, we simply say that  $x = 0$  is trajectory). Similarly, we can get that  $x = 0$  is the trajectory of (13).

By (12), we get that

$$\left(\frac{x}{c_1}\right)^{\mu/(1-\mu+\mu\alpha)} = \left(\frac{y}{c_2}\right)^{\lambda/(1-\lambda+\lambda\alpha)} \quad \text{or } y = cx^{\mu(1-\lambda+\lambda\alpha)/(\lambda(1-\mu+\mu\alpha))}. \quad (17)$$

where  $c$  is an arbitrary constant.

The picture of all trajectories of a system is called the phase portrait of the system. Since the solutions of (8) can be determined explicitly, a complete description of its phase portrait can be given. However, as we have seen earlier, the nature of the solutions of (8) depends on the eigenvalues of the matrix  $A$ . Thus, the phase portrait of (8) depends almost entirely on the values of  $\lambda$  and  $\mu$ . For this, there are several different cases which must be studied separately. In the following, we investigate the case  $\mathcal{L}$  and construct the phase portraits of system (8). Since  $\det(A) \neq 0$ , it follows that  $\lambda\mu \neq 0$ ; thus, we will consider three cases as follows.

*Case 1.*  $\lambda = \mu$ .

If  $\lambda = \mu$ , it follows that  $y = cx$ . Therefore, the trajectories are half-lines leaving or entering singular point  $O(0, 0)$ . By (12), if  $\lambda < 0$ , then  $\lambda\alpha/(1 - \lambda + \lambda\alpha) = \mu\alpha/(1 - \mu + \mu\alpha) < 0$ . Thus, both  $x(t)$  and  $y(t)$  tend to zero as  $t \rightarrow +\infty$  (singular point  $O(0, 0)$  is called stable node). If  $\lambda > 0$ , however, there are two cases occur as the different selection of  $\alpha$ . The two cases are  $\lambda\alpha/(1 - \lambda + \lambda\alpha) = \mu\alpha/(1 - \mu + \mu\alpha) < 0$  and  $0 < \lambda\alpha/(1 - \lambda + \lambda\alpha) = \mu\alpha/(1 - \mu + \mu\alpha)$ . If  $\lambda\alpha/(1 - \lambda + \lambda\alpha) = \mu\alpha/(1 - \mu + \mu\alpha) < 0$ , then the result is the same as  $\lambda < 0$ . If  $0 < \lambda\alpha/$

$1 - \lambda + \lambda\alpha) = \mu\alpha/(1 - \mu + \mu\alpha)$ , then all solutions tend to  $+\infty$  as  $t \rightarrow +\infty$  (singular point  $O(0, 0)$  is called unstable node). The phase portraits of this case can be found in Example 1.

In the following cases, we assume that  $\lambda \neq \mu$  and consider Case 2 and Case 3.

*Case 2.  $\lambda\mu > 0$ .*

In this case, we will consider two subcases, that is  $\lambda < 0$  and  $\mu < 0$  or  $\lambda > 0$  and  $\mu > 0$ .

Subcase 1.  $\lambda < 0$  and  $\mu < 0$

We may assume that  $\mu < \lambda < 0$  (otherwise, we can exchange  $x$  and  $y$ ). Thus, we get that  $(\mu(1 - \lambda + \lambda\alpha))/(\lambda(1 - \mu + \mu\alpha)) > 1$ . Otherwise,  $(\mu(1 - \lambda + \lambda\alpha))/(\lambda(1 - \mu + \mu\alpha)) \leq 1$ ; this implies that  $\mu \geq \lambda$ , a contradiction. By (17), the trajectories are a family of parabolas which tangent to the  $x$ -axis at the origin, except  $x = 0$  and  $y = 0$ . And both  $x(t)$  and  $y(t)$  tend to zero as  $t \rightarrow +\infty$  (singular point  $O(0, 0)$  is called stable node).

Subcase 2.  $\lambda > 0$  and  $\mu > 0$

We may assume that  $\lambda > \mu > 0$  (otherwise, we can exchange  $x$  and  $y$ ). In this subcase, one of the following holds.

- (i)  $(\mu(1 - \lambda + \lambda\alpha))/(\lambda(1 - \mu + \mu\alpha)) > 1$ . This implies that  $1 - \lambda + \lambda\alpha < 0$  and  $1 - \mu + \mu\alpha < 0$
- (ii)  $0 < (\mu(1 - \lambda + \lambda\alpha))/(\lambda(1 - \mu + \mu\alpha)) < 1$ . This implies that  $1 - \lambda + \lambda\alpha > 0$  and  $1 - \mu + \mu\alpha > 0$
- (iii)  $(\mu(1 - \lambda + \lambda\alpha))/(\lambda(1 - \mu + \mu\alpha)) < 0$ . This implies that  $1 - \lambda + \lambda\alpha < 0$  and  $1 - \mu + \mu\alpha > 0$

For (i) of Subcase 2 of Case 2, by (17), the trajectories are a family of parabolas which tangent to the  $x$ -axis at the origin (stable node), except  $x = 0$  and  $y = 0$ . For (ii) of Subcase 2 of Case 2, by (17), the trajectories are a family of parabolas which tangent to the  $y$ -axis at the origin (unstable node), except  $x = 0$  and  $y = 0$ . For (iii) of Subcase 2 of Case 2, by (17), except  $x = 0$  and  $y = 0$ , the trajectories are a family of hyperbolas which take  $x = 0$  and  $y = 0$  as asymptotes. In this case,  $(x(t), y(t))$  will stay away from  $(0, 0)$  as  $t \rightarrow +\infty$ , and the origin is called saddle point which is unstable.

The phase portraits of Case 2 can be found in Example 2.

*Case 3.  $\lambda\mu < 0$ .*

In this case, we will consider two subcases, that is,  $\lambda > 0 > \mu$  or  $\lambda < 0 < \mu$ .

Subcase 1.  $\lambda > 0 > \mu$

In this subcase, one of the following holds.

- (i)  $\lambda\alpha/(1 - \lambda + \lambda\alpha) < 0$  and  $\mu\alpha/(1 - \mu + \mu\alpha) < 0$
- (ii)  $\lambda\alpha/(1 - \lambda + \lambda\alpha) > 0$  and  $\mu\alpha/(1 - \mu + \mu\alpha) < 0$

For (i) of Subcase 1 of Case 3, by (17), the trajectories are a family of parabolas which tangent to the  $y$ -axis at the origin (stable node), except  $x = 0$  and  $y = 0$ . For (ii) of Subcase 1 of Case 3, by (17), except  $x = 0$  and  $y = 0$ , the trajectories are

a family of hyperbolas which take  $x = 0$  and  $y = 0$  as asymptotes. In this case,  $(x(t), y(t))$  will stay away from  $(0, 0)$  as  $t \rightarrow -\infty$ , and the origin is called saddle point which is unstable. The phase portraits of this case can be found in Example 3.

Subcase 2.  $\lambda < 0 < \mu$

In this subcase, one of the following holds.

- (i)  $\mu\alpha/(1 - \mu + \mu\alpha) < 0$  and  $\lambda\alpha/(1 - \lambda + \lambda\alpha) < 0$
- (ii)  $\mu\alpha/(1 - \mu + \mu\alpha) > 0$  and  $\lambda\alpha/(1 - \lambda + \lambda\alpha) < 0$

For Subcase 2 of Case 3, the analysis is similar to Subcase 1 of Case 3. For (i) of Subcase 2 of Case 3, by (17), the trajectories are a family of parabolas which tangent to the  $y$ -axis at the origin (stable node), except  $x = 0$  and  $y = 0$ . For (ii) of Subcase 2 of Case 3, by (17), except  $x = 0$  and  $y = 0$ , the trajectories are a family of hyperbolas which take  $x = 0$  and  $y = 0$  as asymptotes. In this case,  $(x(t), y(t))$  will stay away from  $(0, 0)$  as  $t \rightarrow +\infty$ , and the origin is called saddle point which is unstable. The phase portraits of this case can be found in Example 4.

We summarize the above analysis in the following theorem for  $A = \mathcal{L}(\lambda, \mu)$ .

**Theorem 4.** For the fractional-order planar autonomous linear system (1), let  $\lambda$  and  $\mu$  be the eigenvalues of the matrix  $A$  with  $a_{12} = a_{21} = 0$ . Then system (1) will become system (8). Then, the behavior of its trajectories near the singular point  $O(0, 0)$  is as follows.

- (i-1) Stable node, if  $\lambda$  and  $\mu$  are equal and negative
- (i-2) Stable node, if  $\lambda$  and  $\mu$  are equal and positive, and  $\lambda\alpha/(1 - \lambda + \lambda\alpha) = \mu\alpha/(1 - \mu + \mu\alpha) < 0$  for some  $\alpha$
- (i-3) Unstable node, if  $\lambda$  and  $\mu$  are equal and positive, and  $\lambda\alpha/(1 - \lambda + \lambda\alpha) = \mu\alpha/(1 - \mu + \mu\alpha) > 0$  for some  $\alpha$
- (ii-1) Stable node, if  $\lambda$  and  $\mu$  are distinct and negative
- (ii-2) Stable node, if  $\lambda$  and  $\mu$  are distinct and positive, and  $(\mu(1 - \lambda + \lambda\alpha))/(\lambda(1 - \mu + \mu\alpha)) > 1$  for some  $\alpha$
- (ii-3) Unstable node, if  $\lambda$  and  $\mu$  are distinct and positive, and  $0 < (\mu(1 - \lambda + \lambda\alpha))/(\lambda(1 - \mu + \mu\alpha)) < 1$  for some  $\alpha$
- (ii-4) Saddle point (unstable), if  $\lambda$  and  $\mu$  are distinct and positive, and  $(\mu(1 - \lambda + \lambda\alpha))/(\lambda(1 - \mu + \mu\alpha)) < 0$  for some  $\alpha$
- (iii-1) Stable node, if  $\lambda$  and  $\mu$  are of opposite sign, and  $(\mu(1 - \lambda + \lambda\alpha))/(\lambda(1 - \mu + \mu\alpha)) > 0$  for some  $\alpha$
- (iii-2) Saddle point (unstable), if  $\lambda$  and  $\mu$  are of opposite sign, and  $(\mu(1 - \lambda + \lambda\alpha))/(\lambda(1 - \mu + \mu\alpha)) < 0$  for some  $\alpha$

In the following, we will consider system (13) and system (15), respectively. For system (13), by Theorem 2, we get that

$$y = (C_1 \ln |x| + C_2)x, \quad (18)$$

where  $C_1 = 1/(\lambda(1 - \lambda + \lambda\alpha))$  and  $C_2 = (c_2/c_1) - (\ln |c_1|/(\lambda(1 - \lambda + \lambda\alpha)))$ . By (18), we know that

$$\lim_{x \rightarrow 0} y = 0 \text{ and } \lim_{x \rightarrow 0} y' = \infty. \quad (19)$$

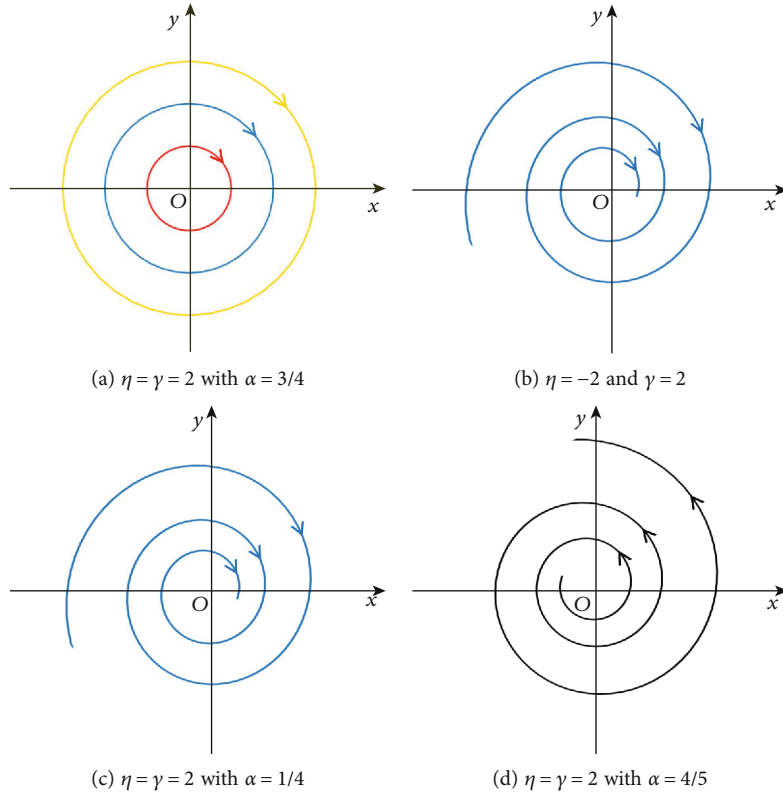


FIGURE 1: The phase portraits of system (15) at different  $\alpha$ .

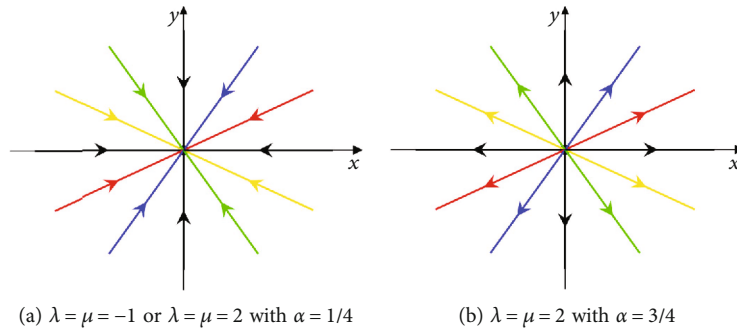


FIGURE 2: The phase portraits of system (8) for  $\lambda = \mu$  at different  $\alpha$ .

Therefore, when the trajectory approaches the origin, the limit position of its tangent is the  $y$ -axis. By Theorem 2, if  $\lambda < 0$ , then  $\lambda\alpha/(1 - \lambda + \lambda\alpha) < 0$ . Thus, as  $t \rightarrow +\infty$ , all trajectories will tend to singular point (singular point  $O(0,0)$  is called stable node). If  $\lambda > 0$ , however, there are two cases occur as the different selection of  $\alpha$ . If  $\lambda\alpha/(1 - \lambda + \lambda\alpha) < 0$ , then the result is the same as  $\lambda < 0$ . If  $\lambda\alpha/(1 - \lambda + \lambda\alpha) > 0$ , then all trajectories will be far away from the singular point as  $t \rightarrow +\infty$  (singular point  $O(0,0)$  is called unstable node). The phase portraits of this case can be found in Example 5.

For system (15), by Theorem 3, we get that

$$\rho = Ce^{-\eta_1 t / \gamma_1}, \tag{20}$$

where  $C = c_1 e^{c_2(\eta_1/\gamma_1)}$ ,  $\eta_1 = (\eta\alpha - (\alpha - \alpha^2)(\eta^2 + \gamma^2)) / ((1 - \eta(1 - \alpha))^2 + \gamma^2(1 - \alpha)^2)$  and  $\gamma_1 = \gamma\alpha / ((1 - \eta(1 - \alpha))^2 + \gamma^2(1 - \alpha)^2)$ . Since  $\gamma > 0$ , we have  $\gamma_1 = \gamma\alpha / ((1 - \eta(1 - \alpha))^2 + \gamma^2(1 - \alpha)^2) > 0$ . If  $\eta_1 = 0$ , by Theorem 3 or (20), we have

$$x^2 + y^2 = c_1^2 \text{ or } \rho = c_1. \tag{21}$$

Thus, the trajectories are closed curves, and the phase portrait of system (15) can be found in Example 6 with  $\eta = \gamma = 2$  and  $\alpha = 3/4$  (see Figure 1(a)). In this case, the singular point  $O(0,0)$  is stable but not asymptotically stable and is called a center.

If  $\eta_1 < 0$ , then the effect of the factor  $e^{\eta_1 t}$  in Theorem 3 is to change the simple closed curves into the spirals. In this



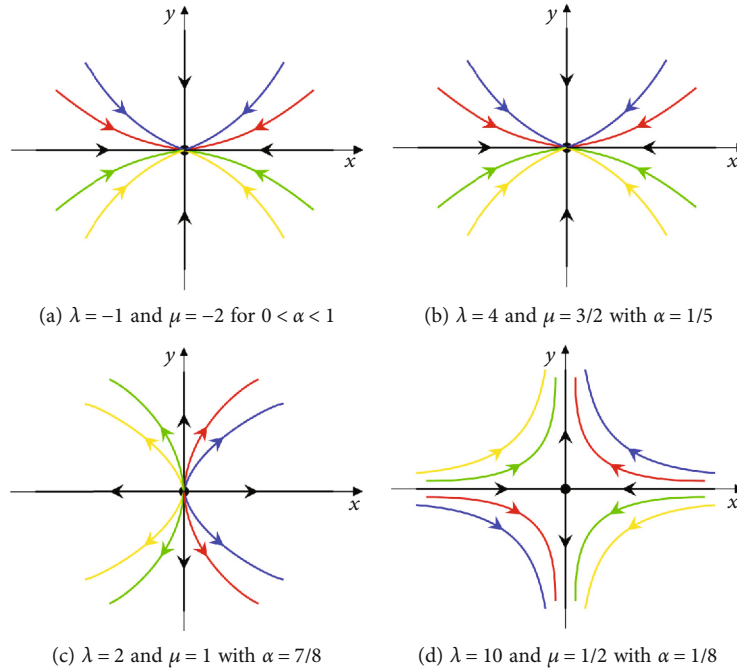


FIGURE 3: The phase portraits of system (8) for  $\lambda \neq \mu$  and  $\lambda\mu > 0$  at different  $\alpha$ .

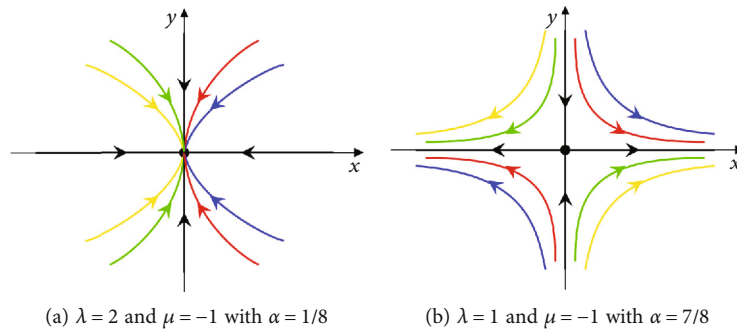


FIGURE 4: The phase portraits of system (8) for  $\lambda > 0 > \mu$  at different  $\alpha$ .

case, the singular point  $O(0,0)$  is asymptotically stable and is called a stable focus. Since  $\eta_1 = (\eta\alpha - (\alpha - \alpha^2)(\eta^2 + \gamma^2)) / ((1 - \eta(1 - \alpha))^2 + \gamma^2(1 - \alpha)^2)$ , we know that if  $\eta < 0$ , then  $\eta_1 < 0$ ; this case can be found in Example 6 with  $\eta = -2$  and  $\gamma = 2$  (see Figure 1(b)). However, if  $\eta \geq 0$ , we also can get  $\eta_1 < 0$  for some values of  $\alpha$ , such as  $\eta = \gamma = 2$  and  $\alpha = 1/4$ , which will be shown in Example 6 (see Figure 1(c)).

If  $\eta_1 > 0$ , then all trajectories of system (15) spiral away from the origin  $O(0,0)$  as  $t \rightarrow +\infty$  and are illustrated in figure of Example 6. This case only happens when  $\eta \geq 0$  for some values of  $\alpha$ , such as  $\eta = \gamma = 2$  and  $\alpha = 4/5$ , which will be shown in Example 6 (see Figure 1(d)). In this case, the singular point  $O(0,0)$  is unstable and is named an unstable focus.

We summarize the above analysis in the following theorem for  $A = \mathcal{M}(\lambda)$  and  $A = \mathcal{R}(\eta, \gamma)$ .

**Theorem 5.** For the fractional-order autonomous linear system (1), let  $\mathcal{M}(\lambda)$  (or  $\mathcal{R}(\eta, \gamma)$ ) be the normal form of matrix

A. Then, the behavior of its trajectories near the singular point  $O(0,0)$  is as follows.

- (i-1) If  $\lambda < 0$ , then  $\lambda\alpha / (1 - \lambda + \lambda\alpha) < 0$  and  $O(0,0)$  is stable node
- (i-2) If  $\lambda > 0$  and  $\lambda\alpha / (1 - \lambda + \lambda\alpha) < 0$  for some  $\alpha$ , then  $O(0,0)$  is stable node
- (i-3) If  $\lambda > 0$  and  $\lambda\alpha / (1 - \lambda + \lambda\alpha) > 0$  for some  $\alpha$ , then  $O(0,0)$  is unstable node
- (ii-1) For  $\eta \geq 0$ , if  $\eta_1 = 0$  at some  $\alpha$ , then  $O(0,0)$  is stable center
- (ii-2) If  $\eta < 0$ , then  $\eta_1 < 0$  and  $O(0,0)$  is stable focus
- (ii-3) For  $\eta \geq 0$ , if  $\eta_1 > 0$  at some  $\alpha$ , then  $O(0,0)$  is stable focus
- (ii-4) For  $\eta \geq 0$ , if  $\eta_1 < 0$  at some  $\alpha$ , then  $O(0,0)$  is unstable focus

#### 4. The Illustrative Examples

In fact, for the classical autonomous systems (9), (14), and (16), the phase portraits can be found in [8, 10]. If the arrow

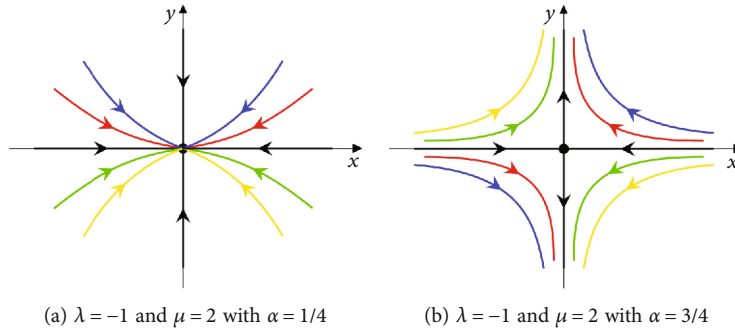


FIGURE 5: The phase portraits of system (8) for  $\lambda < 0 < \mu$  at different  $\alpha$ .

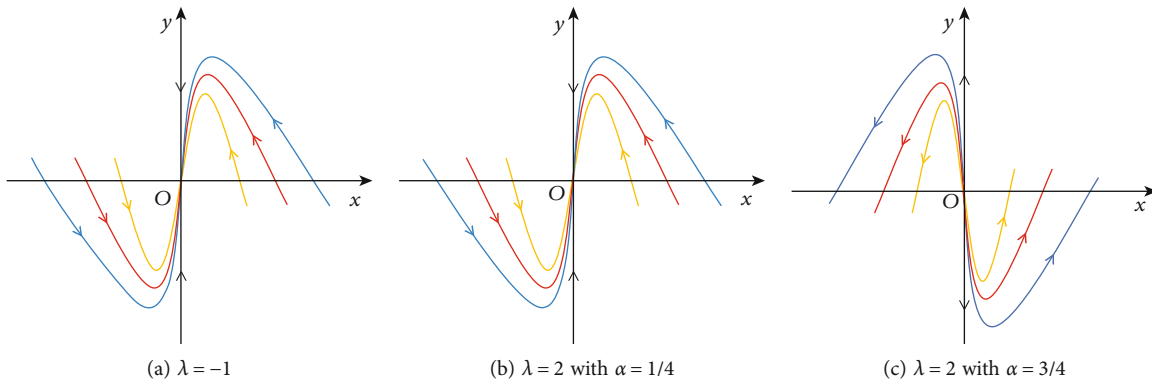


FIGURE 6: The phase portraits of system (13) at different  $\alpha$ .

is pointing to the singular point, then the singular point  $O(0, 0)$  is a stable point; otherwise, it is an unstable point. Next, we make a detailed analysis of  $A = \mathcal{L}(\lambda, \mu)$ ; the results will be shown in Examples 1-4. For  $A = \mathcal{M}(\lambda)$  and  $A = \mathcal{R}(\eta, \gamma)$ , we can get similar results as in Example 5 and Example 6, respectively.

For  $A = \mathcal{L}(\lambda, \mu)$ , there are three cases as analyzed in Section 3. For case  $\lambda = \mu$ , comparing our results with those in [8, 10], we can find that the results of system (8) and system (9) are consistent for the case  $\lambda = \mu < 0$ . However, the results of the case  $\lambda = \mu > 0$  are inconsistent. For  $\lambda = \mu > 0$  of classical autonomous system (9), the results can be found as the same one in Example 1 Figure 2(b). For  $\lambda = \mu > 0$  of system (8), if  $\lambda\alpha/(1 - \lambda + \lambda\alpha) = \mu\alpha/(1 - \mu + \mu\alpha) < 0$ , then the result is the same as  $\lambda < 0$  in Example 1 Figure 2(a), and if  $\lambda\alpha/(1 - \lambda + \lambda\alpha) = \mu\alpha/(1 - \mu + \mu\alpha) > 0$ , then the result can be found in Example 1 Figure 2(b).

For case  $\lambda \neq \mu$  and  $\lambda\mu > 0$ , the results of system (8) and system (9) are inconsistent. Precisely speaking, for case  $\lambda\mu > 0$ , the trajectories of classical autonomous system (9) are a family of parabolas; they all can be found in [8, 10]. However, for case  $\lambda\mu > 0$ , the trajectories of system (8) may be a family of parabolas or hyperbolas as the different selection of  $\alpha$ . As the results in Examples 2, if  $(\mu(1 - \lambda + \lambda\alpha))/(\lambda(1 - \mu + \mu\alpha)) > 0$  for some  $\alpha$ , then the results are shown in Figures 3(a)-3(c); the trajectories of system (8) are a family of parabolas. If  $(\mu(1 - \lambda + \lambda\alpha))/(\lambda(1 - \mu + \mu\alpha)) < 0$  for some  $\alpha$ , then the result is shown in Figure 3(d); the trajectories of system (8) are a family of hyperbolas.

Similarly, for case  $\lambda\mu < 0$ , the results of system (8) and system (9) are also inconsistent. Precisely speaking, for case  $\lambda\mu < 0$ , the trajectories of classical autonomous system (9) are a family of hyperbolas; they all can be found in [8, 10]. However, for case  $\lambda\mu < 0$ , the trajectories of system (8) may be a family of parabolas or hyperbolas as the different selection of  $\alpha$ ; the results can be found in Examples 3 and 4. If  $(\mu(1 - \lambda + \lambda\alpha))/(\lambda(1 - \mu + \mu\alpha)) > 0$  for some  $\alpha$ , then the results are shown in Figures 4(a) and 5(a); the trajectories of system (8) are a family of parabolas. If  $(\mu(1 - \lambda + \lambda\alpha))/(\lambda(1 - \mu + \mu\alpha)) < 0$  for some  $\alpha$ , then the results are shown in Figures 4(b) and 5(b); the trajectories of system (8) are a family of hyperbolas.

*Example 1.* In this example, we consider the case for  $\lambda = \mu \neq 0$ . For  $\lambda = \mu = -1$  or  $\lambda = \mu = 2$  with  $\alpha = 1/4$ , the results can be found in Figure 2(a), which verify (i-1) and (i-2) in Theorem 4. The results of  $\lambda = \mu = 2$  with  $\alpha = 3/4$  can be found in Figure 2(b), which verify (i-3) in Theorem 4. From Figure 2, it can be seen that our results of Case 1 are consistent with the analysis in Section 3.

*Example 2.* The second example is for Case 2 in Section 3. For Subcase 1 of Case 2, if  $\lambda = -1$  and  $\mu = -2$ , then the results can be found in Figure 3(a), which verify (ii-1) in Theorem 4. If  $\lambda = 4$  and  $\mu = 3/2$  with  $\alpha = 1/5$ , then Figure 3(b) is for Subcase 2 (i) of Case 2, which verify (ii-2) in Theorem 4. If  $\lambda = 2$  and  $\mu = 1$  with  $\alpha = 7/8$ , then Figure 3(c) is for Subcase 2 (ii) of Case 2, which verify (ii-3) in Theorem 4. If  $\lambda = 10$

and  $\mu = 1/2$  with  $\alpha = 1/8$ , then Figure 3(d) is for Subcase 2 (iii) of Case 2, which verify (ii-4) in Theorem 4. From Figure 3, it can be seen that our results of Case 2 are consistent with the analysis in Section 3.

*Example 3.* The third example is for Subcase 1 of Case 3 in Section 3. If  $\lambda = -2$  and  $\mu = -1$  with  $\alpha = 1/8$ , then Figure 4(a) is for Subcase 1 (i) of Case 3, which verify (iii-1) in Theorem 4. If  $\lambda = 1$  and  $\mu = -1$  with  $\alpha = 7/8$ , then Figure 4(b) is for Subcase 1 (ii) of Case 3, which verify (iii-2) in Theorem 4. From Figure 4, it can be seen that our results of Subcase 1 of Case 3 are consistent with the analysis in Section 3.

*Example 4.* The fourth example is for Subcase 2 of Case 3 in Section 3. If  $\lambda = -1$  and  $\mu = 2$  with  $\alpha = 1/4$ , then Figure 5(a) is for Subcase 2 (i) of Case 3, which verify (iii-1) in Theorem 4. If  $\lambda = -1$  and  $\mu = 2$  with  $\alpha = 3/4$ , then Figure 5(b) is for Subcase 2 (ii) of Case 3, which verify (iii-2) in Theorem 4. From Figure 5, it can be seen that our results of Subcase 2 of Case 3 are consistent with the analysis in Section 3.

*Example 5.* In this example, we consider the phase portraits for system (13). For  $\lambda = -1$ , the result can be found in Figure 6(a), which verify (i-1) in Theorem 5. For  $\lambda = 2$  with  $\alpha = 1/4$ , the result can be found in Figure 6(b), which verify (i-2) in Theorem 5. The result of  $\lambda = 2$  with  $\alpha = 3/4$  can be found in Figure 6(c), which verify (i-3) in Theorem 5. From Figure 6, it can be found that our results are consistent with the analysis in Section 3.

*Example 6.* This example is for system (15). If  $\eta = \gamma = 2$  with  $\alpha = 3/4$ , then the results can be found in Figure 1(a), which verify (ii-1) in Theorem 5. If  $\eta = -2$  and  $\gamma = 2$ , then the results can be found in Figure 1(b), which verify (ii-2) in Theorem 5. If  $\eta = \gamma = 2$  with  $\alpha = 1/4$ , then the results can be found in Figure 1(c), which verify (ii-3) in Theorem 5. If  $\eta = \gamma = 2$  with  $\alpha = 4/5$ , then the results can be found in Figure 1(d), which verify (ii-4) in Theorem 5. From Figure 1, it can be seen that our results are consistent with the analysis in Section 3.

## 5. Conclusion

In this paper, we study the trajectories and singular points for two-dimensional fractional-order planar autonomous linear systems involving the Caputo-Fabrizio fractional derivative. This problem is a natural generalization of the classical autonomous systems. Compared with the classical integer-order autonomous systems, trajectories of the solutions for fractional-order autonomous systems have more abundant physical phenomena. The results of our paper will further enrich the related contents of fractional-order autonomous systems. In the future, fractional-order complex autonomous systems and fractional-order autonomous nonlinear systems can also be studied.

## Data Availability

Data sharing is not applicable to this article as no datasets were generated or analyzed during the current study.

## Conflicts of Interest

The authors declare that they have no conflicts of interest.

## Acknowledgments

This work is supported by the Natural Science Foundation of Xinjiang Uygur Autonomous Region (No. 2022D01E13), the National Natural Science Foundation of China (No. 11861068 and No. 11761071), Guizhou Key Laboratory of Big Data Statistical Analysis, China (No. [2019]5103), and the Scientific Research Foundation for Outstanding Young Teachers of Xinjiang Normal University, China (No. XJNU202012 and No. XJNU202112).

## References

- [1] I. Podlubny, *Fractional Differential Equations*, Academic Press, San Diego, CA, 1999.
- [2] R. B. Albadarneh, I. M. Batiha, A. Adwai, N. Tahat, and A. K. Alomari, "Numerical approach of Riemann-Liouville fractional derivative operator," *International Journal of Electrical and Computer Engineering (IJECE)*, vol. 11, no. 6, pp. 5367–5378, 2021.
- [3] R. B. Albadarneh, I. Batiha, A. K. Alomari, and N. Tahat, "Numerical approach for approximating the Caputo fractional-order derivative operator," *AIMS Mathematics*, vol. 6, no. 11, pp. 12743–12756, 2021.
- [4] Y. M. Lin and C. J. Xu, "Finite difference/spectral approximations for the time-fractional diffusion equation," *Journal of Computational Physics*, vol. 225, no. 2, pp. 1533–1552, 2007.
- [5] P. Zhuang, F. Liu, V. Anh, and I. Turner, "Numerical methods for the variable-order fractional advection diffusion equation with a nonlinear source term," *SIAM Journal on Numerical Analysis*, vol. 47, no. 3, pp. 1760–1781, 2009.
- [6] J. J. Nieto, "Solution of a fractional logistic ordinary differential equation," *Applied Mathematics Letters*, vol. 123, article 107568, 2022.
- [7] J. Liu, J. Zhang, and X. D. Zhang, "Semi-discretized numerical solution for time fractional convection-diffusion equation by RBF-FD," *Applied Mathematics Letters*, vol. 128, article 107880, 2022.
- [8] W. Walter, *Ordinary Differential Equations*, Springer-verlag New York, 1998.
- [9] S. P. Bhaty and D. S. Bernstein, "Finite-time stability of continuous autonomous systems," *SIAM Journal on Control and Optimization*, vol. 38, no. 3, pp. 751–766, 2000.
- [10] R. P. Agarwal and D. O'Regan, *An Introduction to Ordinary Differential Equations*, Springer Science Business Media LLC, 2008.
- [11] J.-C. Cortés, A. Navarro-Quiles, J.-V. Romero, and M.-D. Roselló, "Full solution of random autonomous first-order linear systems of difference equations. Application to construct random phase portrait for planar systems," *Applied Mathematics Letters*, vol. 68, pp. 150–156, 2017.



- [12] R. B. Albadarneh, I. M. Batiha, N. Tahat, and A. K. Alomari, "Analytical solutions of linear and non-linear incommensurate fractional-order coupled systems," *Indonesian Journal of Electrical Engineering and Computer Science*, vol. 21, no. 2, pp. 776–790, 2021.
- [13] W. M. Ahmad and W. M. Harb, "On nonlinear control design for autonomous chaotic systems of integer and fractional orders," *Chaos, Solitons & Fractals*, vol. 18, no. 4, pp. 693–701, 2003.
- [14] C. G. Li and G. R. Chen, "Chaos in the fractional order Chen system and its control," *Chaos, Solitons & Fractals*, vol. 22, no. 3, pp. 549–554, 2004.
- [15] S. T. Kingni, V.-T. Pham, S. Jafari, G. R. Kol, and P. Wofofo, "Three-dimensional chaotic autonomous system with a circular equilibrium: analysis, circuit implementation and its fractional-order form," *Circuits, Systems, and Signal Processing*, vol. 35, no. 6, pp. 1933–1948, 2016.
- [16] M. Caputo and M. Fabrizio, "A new definition of fractional derivative without singular kernel," *Progress in Fractional Differentiation & Applications*, vol. 1, pp. 73–78, 2015.
- [17] J. Losada and J. J. Nieto, "Properties of a new fractional derivative without singular kernel," *Progress in Fractional Differentiation and Applications*, vol. 1, pp. 87–92, 2015.
- [18] J. Losada and J. J. Nieto, "Fractional integral associated to fractional derivatives with nonsingular kernels," *Progress in Fractional Differentiation and Applications*, vol. 7, pp. 137–143, 2021.
- [19] T. Akman, B. Yildiz, and D. Baleanu, "New discretization of Caputo-Fabrizio derivative," *Computational and Applied Mathematics*, vol. 37, no. 3, pp. 3307–3333, 2018.
- [20] M. Z. Xu and Y. J. Jian, "Unsteady rotating electroosmotic flow with time-fractional Caputo-Fabrizio derivative," *Applied Mathematics Letters*, vol. 100, article 106015, 2020.
- [21] M. Caputo and M. Fabrizio, "On the singular kernels for fractional derivatives. Some applications to partial differential equations," *Progress in Fractional Differentiation and Applications*, vol. 7, pp. 79–82, 2021.
- [22] K. M. Owolabi, "Computational analysis of different Pseudoplattystoma species patterns the Caputo-Fabrizio derivative," *Chaos, Solitons & Fractals*, vol. 144, article 110675, 2021.
- [23] F. Haq, I. Mahariq, T. Abdeljawad, and N. Maliki, "A new approach for the qualitative study of vector born disease using Caputo-Fabrizio derivative," *Numerical Methods for Partial Differential Equations*, vol. 37, no. 2, pp. 1809–1818, 2021.
- [24] M. Fardi and Y. Khan, "A novel finite difference-spectral method for fractal mobile/immobile transport model based on Caputo-Fabrizio derivative," *Chaos, Solitons & Fractals*, vol. 143, article 110573, 2021.
- [25] N. Harrouche, S. Momani, S. Hasan, and M. Al-Smadi, "Computational algorithm for solving drug pharmacokinetic model under uncertainty with nonsingular kernel type Caputo-Fabrizio fractional derivative," *Alexandria Engineering Journal*, vol. 60, no. 5, pp. 4347–4362, 2021.
- [26] T. W. Zhang and Y. K. Li, "Exponential Euler scheme of multi-delay Caputo-Fabrizio fractional-order differential equations," *Applied Mathematics Letters*, vol. 124, article 107709, 2022.
- [27] S. Bhalekar and M. Patil, "Singular points in the solution trajectories of fractional order dynamical systems," *Chaos*, vol. 28, no. 11, article 113123, 2018.
- [28] G. Reißig and H. Boche, "Straightening out trajectories near singular points of implicit differential equations," in *Proc. 9th Int. Symp. System-Modelling-Control (SMC)*, Zakopane, PL, 1998.
- [29] Z. Bilicki, C. Dafermos, J. Kestin, G. Majda, and D. L. Zeng, "Trajectories and singular points in steady-state models of two-phase flows," *International journal of multiphase flow*, vol. 13, no. 4, pp. 511–533, 1987.
- [30] S. Wang, J. Liu, and X. D. Zhang, "Properties of solutions for fractional-order linear system with differential equations," *AIMS Mathematics*, vol. 7, no. 8, pp. 15704–15713, 2022.